Electronic Supplementary Material (ESI) for Dalton Transactions.
This journal is © The Royal Society of Chemistry 2019

Correlating magnetic anisotropy and $[Mo(CN)_7]^{4-}$ geometry of Mn^{II}-Mo^{III} magnetic frameworks

Michał Magott,[a] Kim R. Dunbar,*[b] Dawid Pinkowicz*[a]

[a]*Jagiellonian University, Gronostajowa 2, 30-348 Kraków, Poland. E-mail: dawid.pinkowicz@uj.edu.pl*

[b]*Department of Chemistry, Texas A&M University, College Station, Texas 77843, USA. E-mail: dunbar@chem.tamu.edu*

Table of Contents

Correlating magnetic anisotropy with [Mo(CN)<inf>7</inf>]^{4−} geometry of Mn^{II}–Mo^{III} magnetic frameworks

1. Experimental details

Single crystal X-ray diffraction. Single crystal X-ray diffraction experiments were performed using a Bruker D8 Quest Eco Photon50 CMOS (**1**, **1Re**, **2** and **3**) or Bruker SMART Apex2 (**4**) diffractometer (MoKα radiation, graphite monochromator). Absorption corrections, data reduction and unit cell refinements were performed using the SADABS and SAINT programs included in the Apex3 suite. The structure was solved using direct methods and refined anisotropically using weighted full-matrix least-squares on F^2.[S1] Hydrogen atoms of the ligands were placed in calculated positions and refined as riders on the parent atoms. Structural diagrams were prepared using Mercury CSD 3.9.[S2]

CCDC 1899234-1899238 contain the supplementary crystallographic data for this paper which can be obtained free of charge from the Cambridge Crystallographic Data Centre via www.ccdc.cam.ac.uk/data_request/cif.

Powder X-ray diffraction. Powder X-ray diffraction (PXRD) data were obtained at room temperature for ground crystalline samples loaded into glass capillaries with the mother liquor (0.5 mm in diameter). The measurements were carried out using a PANalytical X'Pert Pro MPD diffractometer (CuKα radiation, graphite monochromator).

Magnetic measurements. Magnetic susceptibility measurements were performed using a Quantum Design MPMS-3 Evercool magnetometer in magnetic fields up to 7 Tesla for samples packed into glass tubes with a small amount of mother liquor. The experimental data were corrected for the diamagnetism of the sample and the sample holder.

IR spectra. IR spectra were recorded using a Nicolet iN10 MX FT-IR microscope in the transmission mode.

2. IR spectra

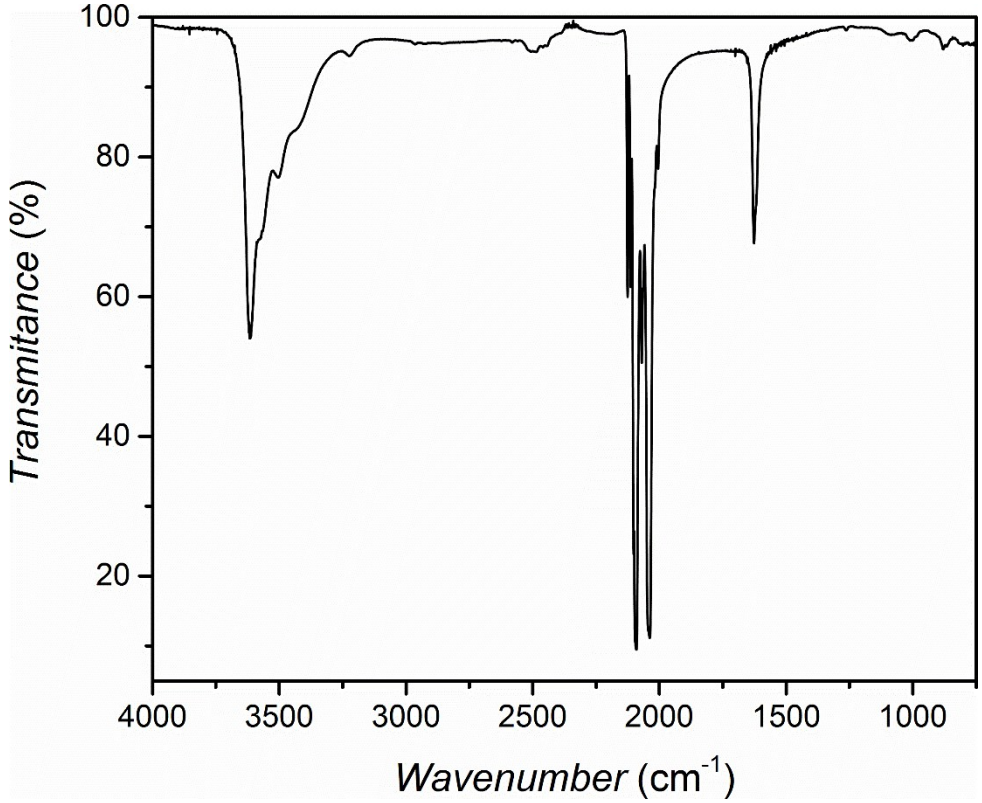

Figure S1. IR spectrum of $K_4[Re^{III}(CN)_7]\cdot 2H_2O$.

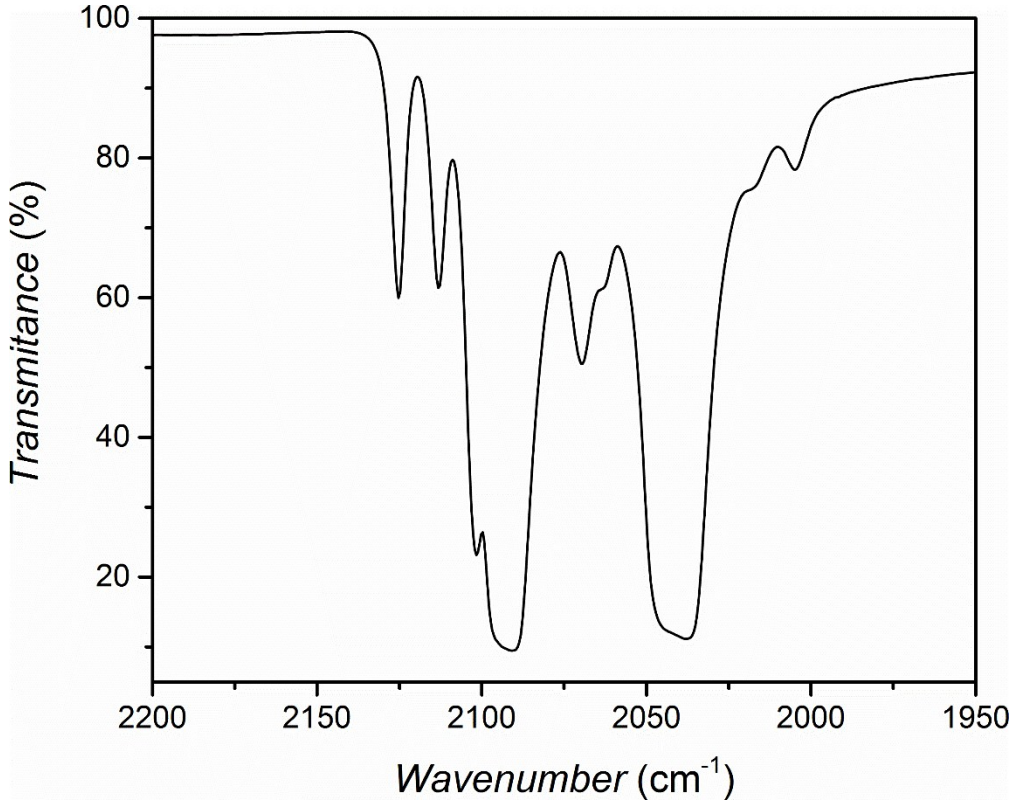

Figure S2. IR spectrum of $K_4[Re^{III}(CN)_7]\cdot 2H_2O$ in the cyanide stretching region.

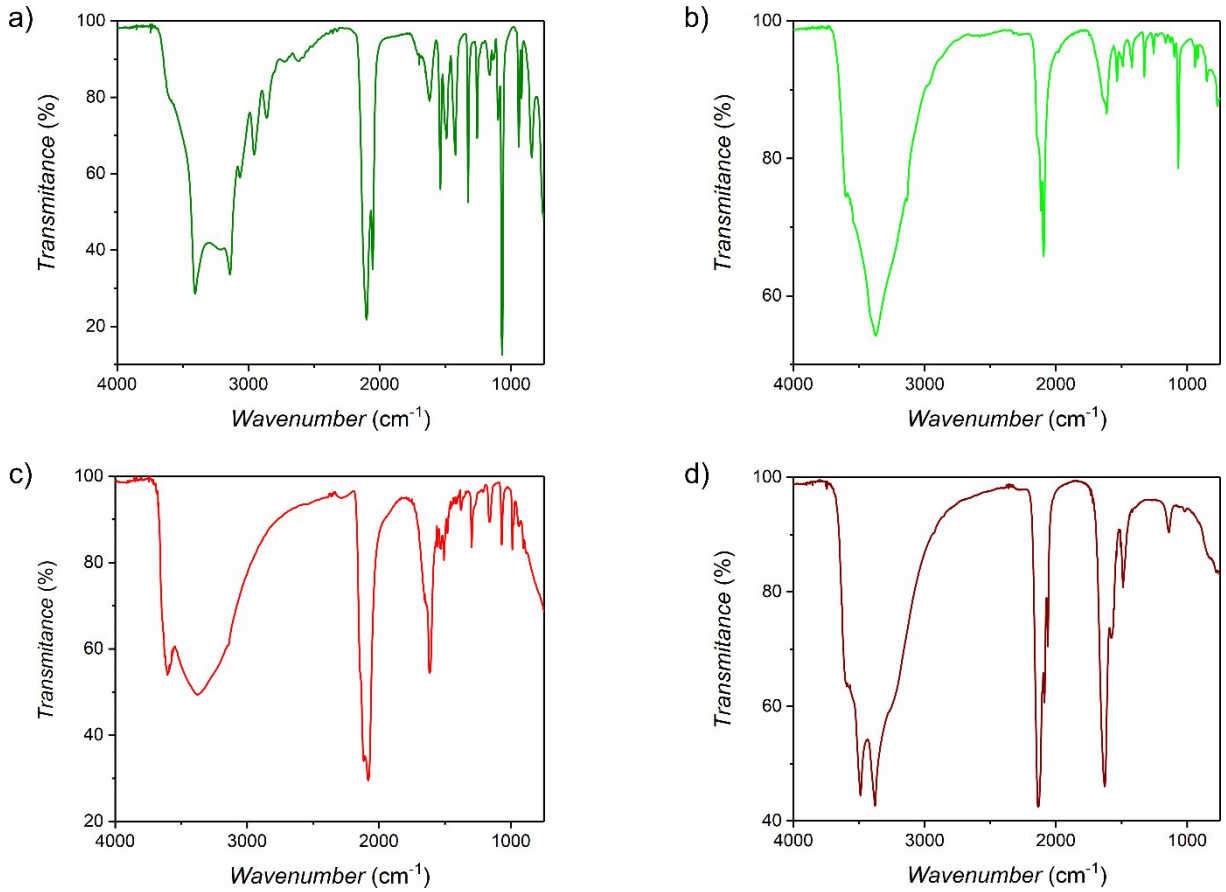

Figure S3. IR spectra of compounds **1-4** (a-d respectively).

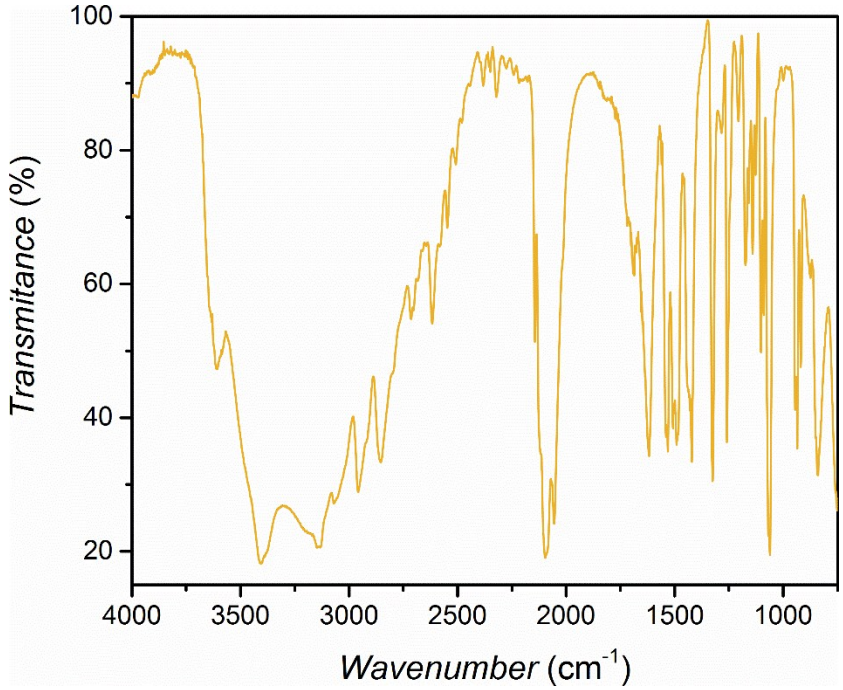

Figure S4. IR spectrum of **1Re**.

3. Powder X-ray diffraction

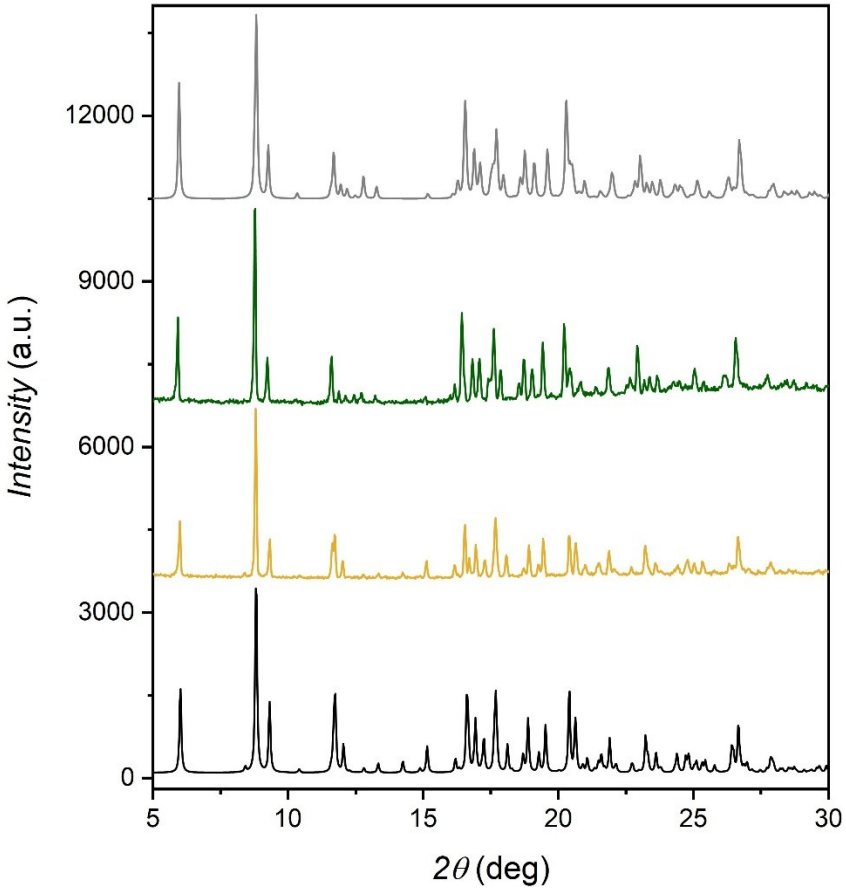

Figure S5. Comparison of the PXRD pattern simulated for single crystals of **1Re** (black line), experimental data obtained for **1Re** (yellow line), experimental data for **1** (green line) and simulated pattern for single crystals of **1** (grey line).

4. Crystal structures

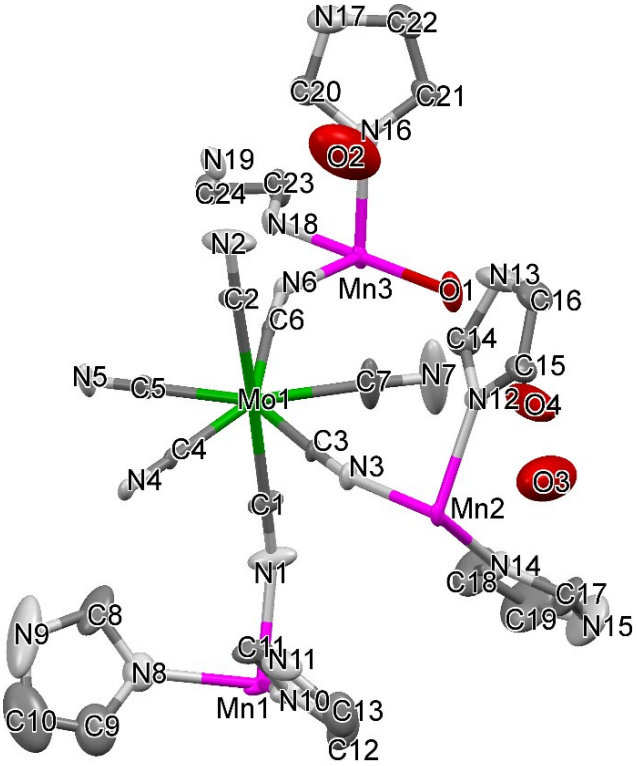

Figure S6. Asymmetric unit of compound **1** (hydrogen atoms were omitted for the sake of clarity). Thermal ellipsoids are depicted at the 30% probability level.

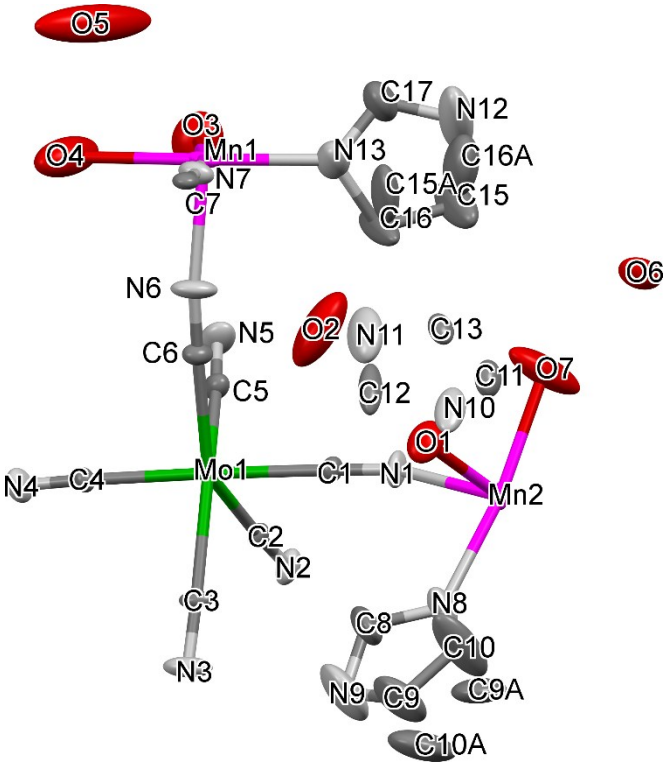

Figure S7. Asymmetric unit of compound **2** (hydrogen atoms were omitted for the sake of clarity). Thermal ellipsoids are depicted at the 50% probability level.

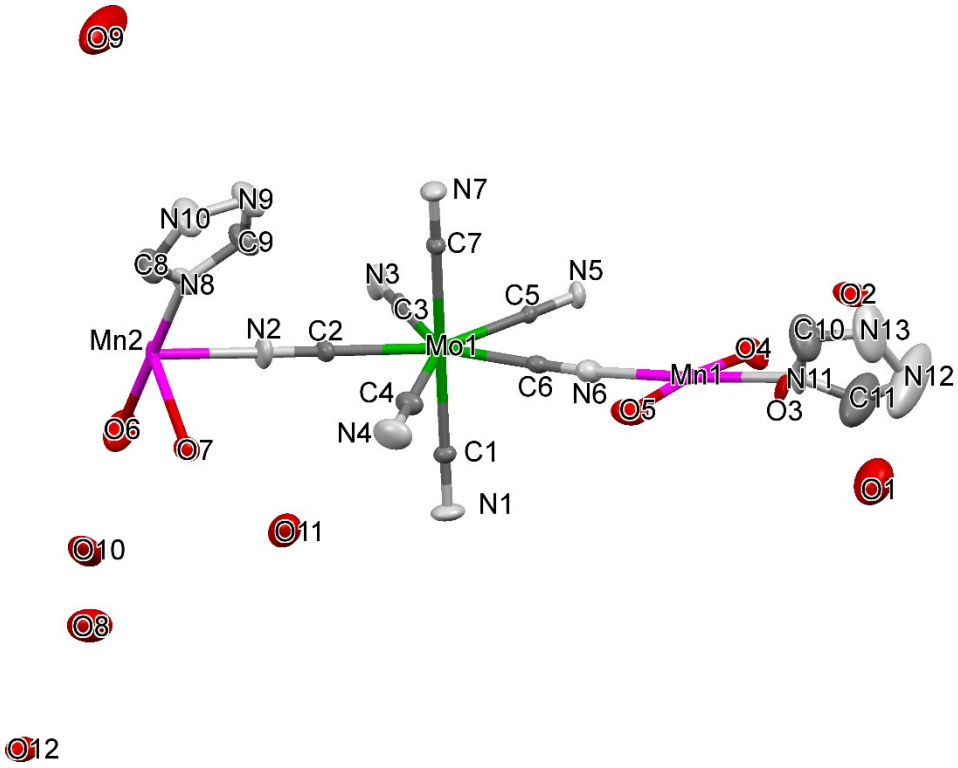

Figure S8. Asymmetric unit of compound **3** (hydrogen atoms were omitted for the sake of clarity). Thermal ellipsoids are depicted at the 50% probability level.

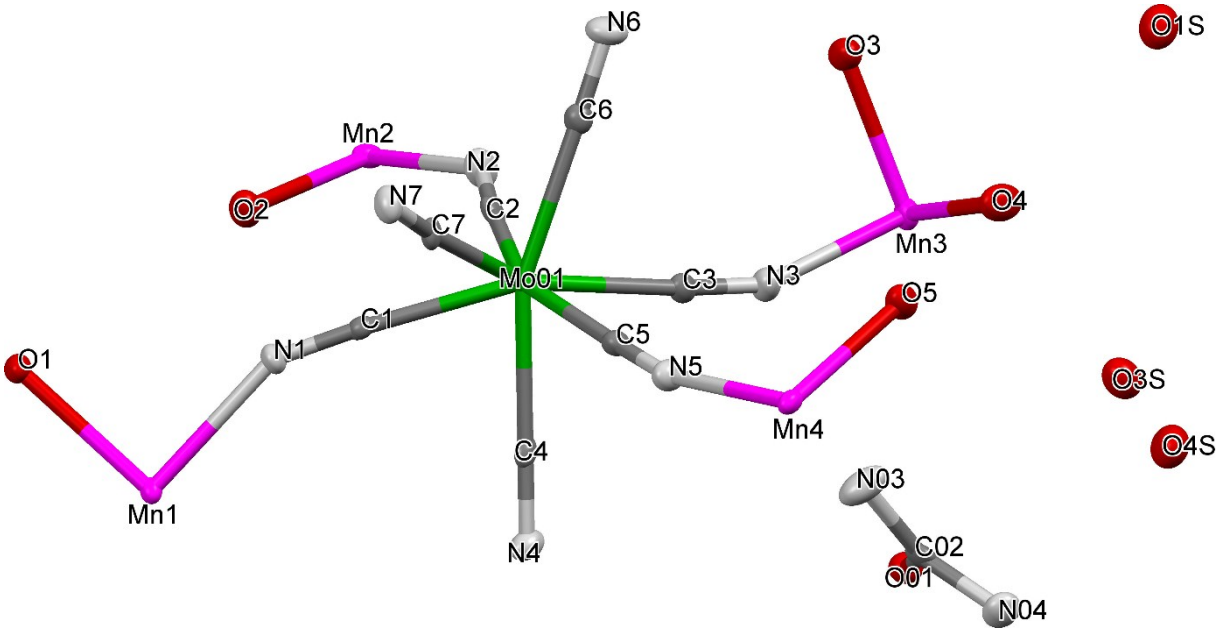

Figure S9. Asymmetric unit of compound **4** (hydrogen atoms were omitted for the sake of clarity). Thermal ellipsoids are depicted at the 50% probability level.

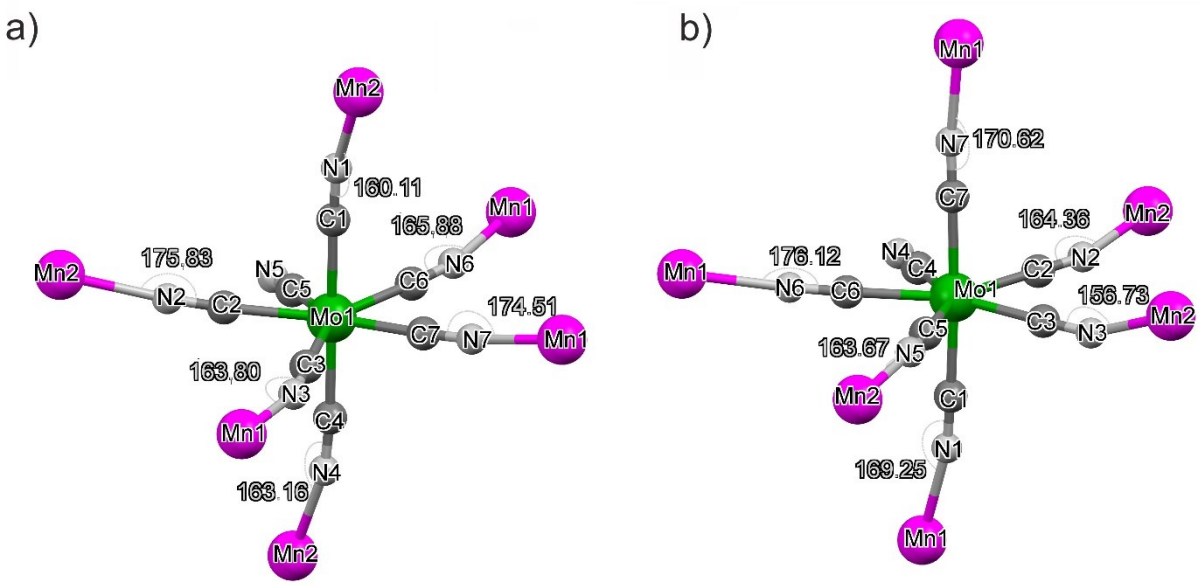

Figure S10. Coordination bridges and Mn-N-C angles in compounds **2** (a) and **3** (b).

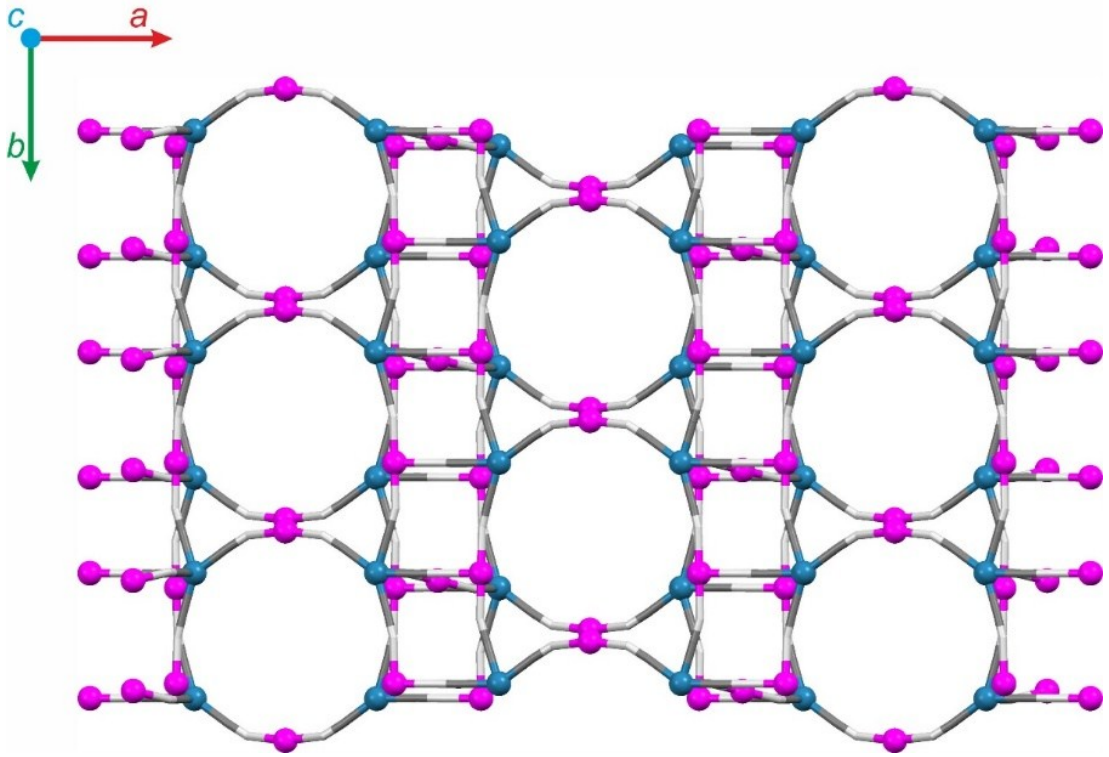

Figure S11. Coordination skeleton of compound **1Re** (blue – rhenium, magenta – manganese) viewed down the *c* axis.

Table S1. Crystallographic data and refinement parameters for compounds **1-4** and **1Re**.[a]

	1	**1Re**
Formula	$C_{47}H_{42}Mn_4Mo_2N_{36}O_7$	$C_{47}H_{40}Mn_4N_{36}O_7Re_2$
FW ($g \cdot mol^{-1}$)	1634.80	1815.32
Temperature (K)	120(2)	120(2)
Crystal system	Monoclinic	Monoclinic
Space group	*C*2/*c*	*C*2/*c*
a (Å)	32.2372(9)	32.116(15)
b (Å)	10.7266(3)	10.630(5)
c (Å)	21.8215(6)	21.932(14)
β (°)	113.426(1)	113.96(2)
V ($Å^3$)	6931.5(3)	6842(6)
Z	4	4
ρ_{calc} ($g \cdot cm^3$)	1.567	1.762
Abs. coeff (mm^{-1})	1.130	4.313
F(000)	3264	3528
Crystal size (mm)	0.20x0.05x0.03	0.38x0.08x0.06
ϑ range (°)	2.67-25.42	2.71-26.79
Reflections collected	32259	33190
R_{int}	0.0688	0.034
Parameters/restraints	448/98	449/98
GOF on F^2	1.041	1.221
R_1 (refl. with I > 2σ(I))	0.0599	0.0481
wR_2 (all reflections)	0.1387	0.1164
Largest diff. peak and hole ($e \cdot Å^{-3}$)	1.171/-0.837	3.29/-1.93
S_{PBPY}	0.129	0.116
S_{CTPR}	5.212	5.488
S_{COC}	6.984	7.159

[a] S_{PBPY}, S_{CTPR}, S_{COC} - shape measure relative to the pentagonal bipyramid (PBPY), capped trigonal prism (CTPR) and capped octahedron (COC). When the shape measure parameter equals zero, the geometry coincides with the idealized one.

Table S1 (continued). Crystallographic data and refinement parameters for compounds **1-4** and **1Re**.

	2	**3**	**4**
Formula	$C_{14.5}Mn_2MoN_{12}O_6$	$C_{10.40}H_{11}Mn_2MoN_{12.10}O_{9.90}$	$C_8H_{20}Mn_2MoN_9O_9$
FW (g·mol^{-1})	644.08	669.73	592.15
Temperature (K)	120(2)	120(2)	150(2)
Crystal system	Triclinic	Triclinic	Triclinic
Space group	$P\bar{1}$	$P\bar{1}$	$P\bar{1}$
a (Å)	10.6308(7)	10.5826(2)	7.239(5)
b (Å)	10.8192(7)	10.9297(2)	12.039(5)
c (Å)	11.8287(8)	12.3540(3)	12.344(5)
α (°)	70.190(3)	67.655(1)	80.062(5)
β (°)	77.920(3)	78.167(1)	89.517(5)
γ (°)	88.094(3)	86.350(1)	89.216(5)
V (Å^3)	1250.59(15)	1293.38(5)	1059.5(10)
Z	2	2	2
ρ_{calc} (g·cm^3)	1.710	1.720	1.856
Abs. coeff (mm^{-1})	1.541	1.504	1.815
F(000)	638	659	590
Crystal size (mm)	0.22x0.12x0.05	0.30x0.30x0.20	0.13x0.06x0.05
ϑ range (°)	2.98-27.16	2.93-27.49	1.67-26.66
Reflections collected	20013	19094	11350
R_{int}	0.035	0.019	0.045
Parameters/restraints	388/19	377/49	348/1
GOF on F^2	1.127	1.062	1.028
R_1 (refl. with I > 2σ(I))	0.0551	0.0332	0.0316
wR_2 (all reflections)	0.1372	0.0837	0.0735
Largest diff. peak and hole (e·Å^{-3})	2.50/-1.39	1.93/-0.84	0.50/-0.49
S_{PBPY}	0.665	0.176	6.660
S_{CTPR}	4.084	5.730	0.650
S_{COC}	5.650	7.371	0.890

[a] S_{PBPY}, S_{CTPR}, S_{COC} - shape measure relative to the pentagonal bipyramid (PBPY), capped trigonal prism (CTPR) and capped octahedron (COC). When the shape measure parameter equals zero, the geometry coincides with the idealized one.

Table S2. Important bond distances (Å) and angles (°) for compounds **1-4** and **1Re** (grey fields denote axial cyanide bridges).

Bond	**1**	**Angle**	**1**
Mn1-N1	2.224(6)	Mn1-N1-C1	151.9(6)
Mn2-N3	2.192(5)	Mn2-N3-C3	166.7(5)
Mn2-N4	2.139(5)	Mn2-N4-C4	177.9(4)
Mn2-N5	2.193(5)	Mn2-N5-C5	162.7(5)
Mn3-N6	2.225(5)	Mn3-N6-C6	149.8(4)
	2		**2**
Mn2-N1	2.185(5)	Mn2-N1-C1	160.1(5)
Mn2-N2	2.211(5)	Mn2-N2-C2	175.8(5)
Mn1-N3	2.166(5)	Mn1-N3-C3	163.8(5)
Mn2-N4	2.206(5)	Mn2-N4-C4	163.2(5)
Mn1-N6	2.180(5)	Mn1-N6-C6	165.9(5)
Mn1-N7	2.177(5)	Mn1-N7-C7	174.5(5)
	3		**3**
Mn1-N1	2.212(3)	Mn1-N1-C1	169.3(3)
Mn2-N2	2.181(3)	Mn2-N2-C2	164.4(3)
Mn2-N3	2.190(3)	Mn2-N3-C3	156.7(3)
Mn2-N5	2.179(2)	Mn2-N5-C5	163.7(2)
Mn1-N6	2.198(3)	Mn1-N6-C6	176.1(2)
Mn1-N7	2.175(2)	Mn1-N7-C7	170.6(3)

Table S2 (continued). Important bond distances (Å) and angles (°) for compounds **1-4** and **1Re** (grey fields denote axial cyanide bridges).

Bond	**4**	**Angle**	**4**
Mn1-N1	2.245(3)	Mn1-N1-C1	152.6(2)
Mn2-N2	2.218(3)	Mn2-N2-C2	142.2(3)
Mn3-N3	2.195(3)	Mn3-N3-C3	158.4(3)
Mn4-N4	2.231(3)	Mn4-N4-C4	154.1(3)
Mn4-N5	2.209(3)	Mn4-N5-C5	166.9(3)
Mn2-N6	2.195(3)	Mn2-N6-C6	149.8(3)
Mn1-N7	2.173(3)	Mn1-N7-C7	157.3(3)
	1Re		**1Re**
Mn1-N1	2.151(6)	Mn1-N1-C1	178.9(7)
Mn1-N2	2.203(8)	Mn1-N2-C2	162.2(7)
Mn3-N3	2.253(7)	Mn3-N3-C3	149.3(7)
Mn2-N6	2.236(10)	Mn2-N6-C6	151.1(8)
Mn1-N7	2.207(7)	Mn1-N7-C7	166.2(7)

5. Magnetic properties

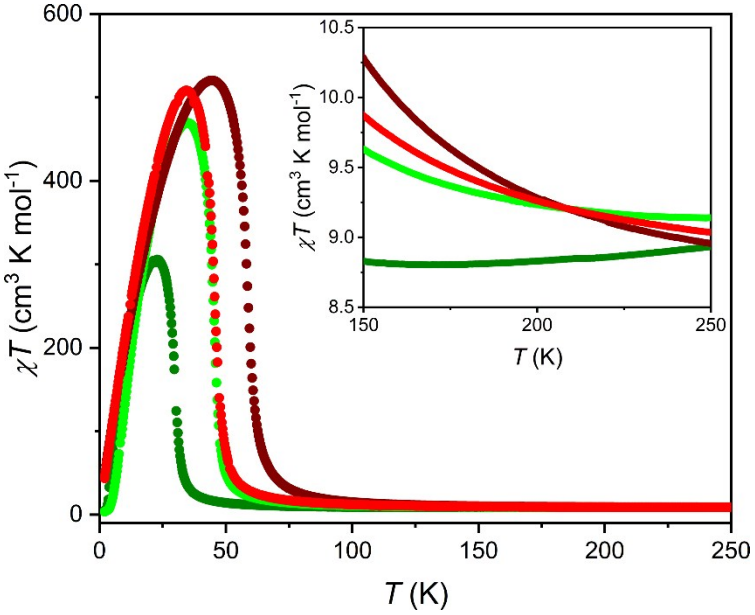

Figure S12. χT versus T plots for compounds **1** (dark green), **2** (light green), **3** (red) and **4** (dark red) at H_{DC} = 1000 Oe. Inset contains a close-up of the 150-250 K region.

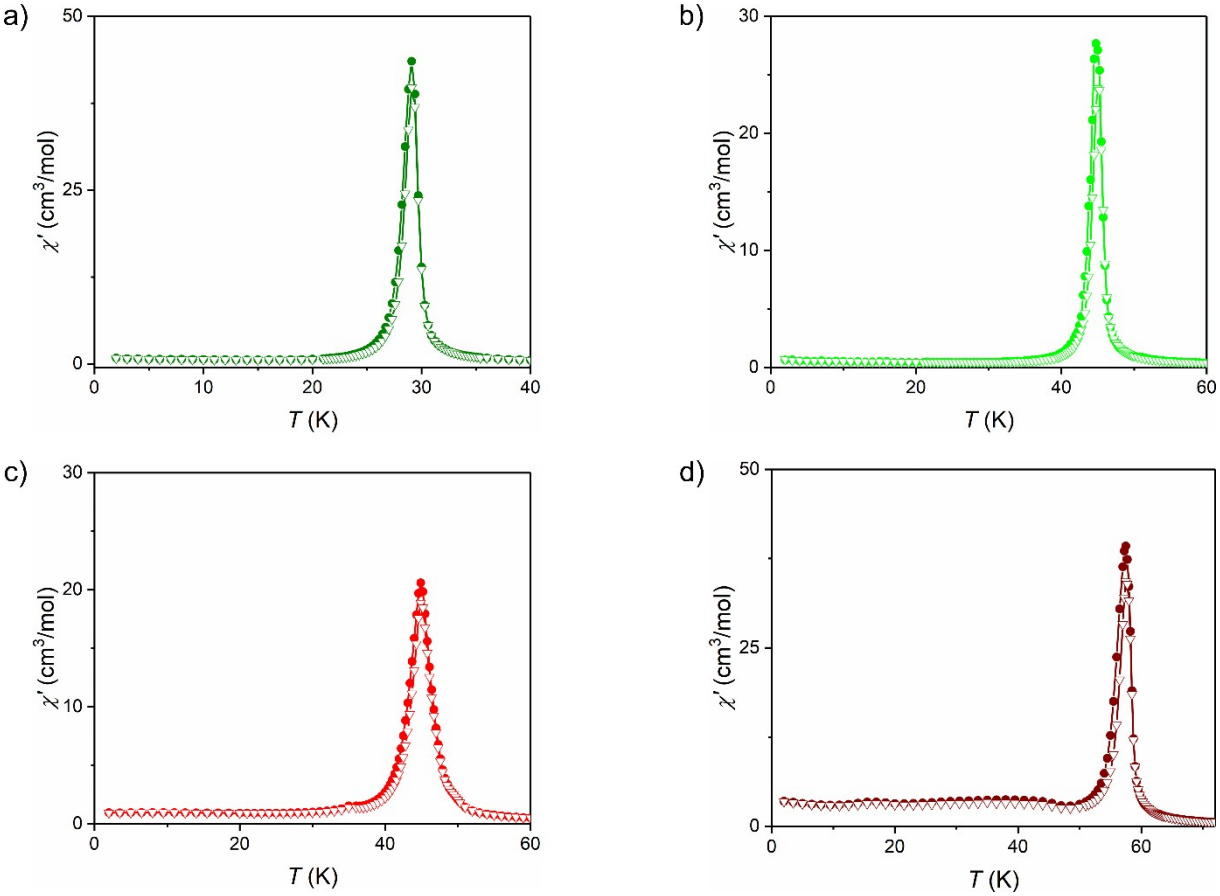

Figure S13. χT versus T plots for compounds **1**-**4** at H_{AC} = 1 Oe and no DC field (a-d respectively; full circles – 70 Hz, open triangles – 700 Hz).

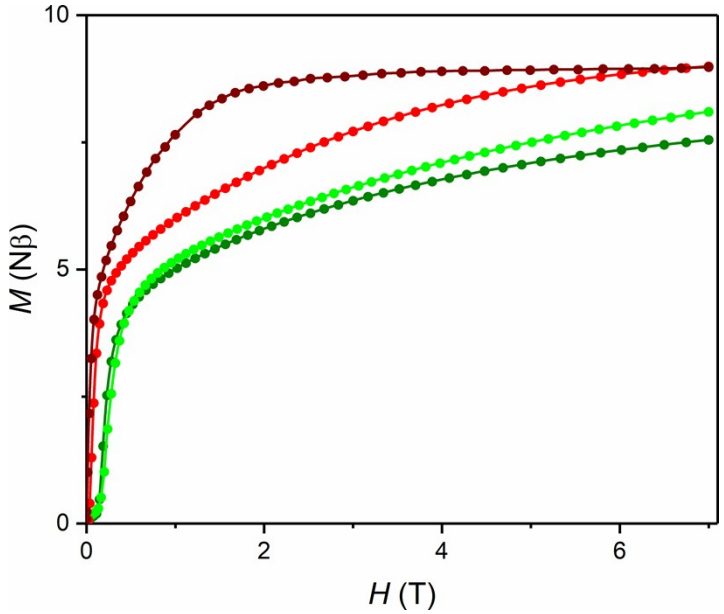

Figure S14. *M* versus *H* plots in the 0-7 T range for compounds **1** (dark green), **2** (light green), **3** (red) and **4** (dark red) at *T* = 1.8 K. Solid lines are guides for an eye.

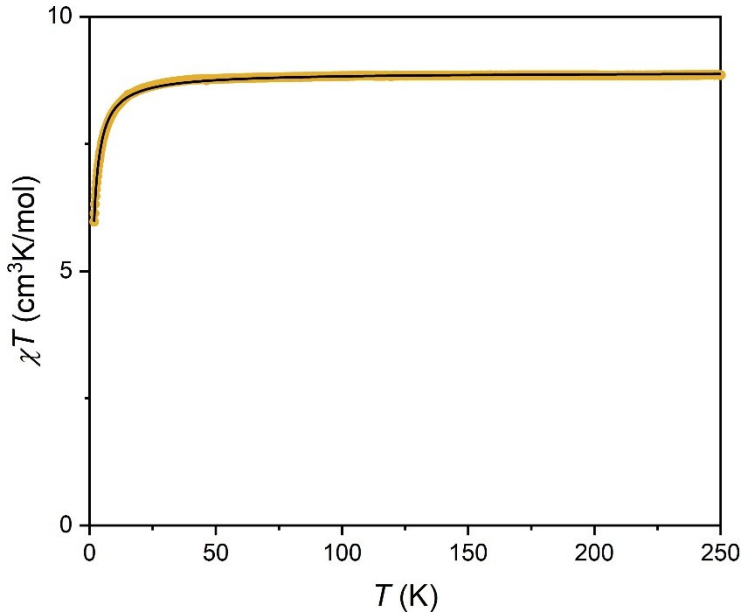

Figure S15. χT versus T plot at *H* = 0.1 T (left) for **1Re**. Yellow points are experimental values and solid line represents the best fit to the mean-field approximation (see details in the manuscript).

References

[S1] a) G. Sheldrick, *Acta Crystallogr., Sect. A: Found. Crystallogr.*, **2008**, *64*, 112 b) G. Sheldrick, *Acta Crystallogr., Sect. C: Struct. Chem.*, **2015**, *71*, 3 c) O. V. Dolomanov, L. J. Bourhis, R. J. Gildea, J. A. K. Howard, H. Puschmann, *J. Appl. Cryst.*, **2009**, *42*, 339

[S2] C. F. Macrae, I. J. Bruno, J. A. Chisholm, P. R. Edgington, P. McCabe, E. Pidcock, L. Rodriguez-Monge, R. Taylor, J. van de Streek, P. A. Wood, *J. Appl. Cryst.*, **2008**, *41*, 466-470